NASA TECHNICAL MEMORANDUM

NASA TM X-73472

NASA TM X-73472

(NASA-TM-X-73472) MODE 1 STRESS INTENSITY FACTORS FOR ROUND COMPACT SPECIMENS (NASA) 7 p HC A02/MF A01 CSCL 20K

N77-10557

Unclas
G3/39 08955

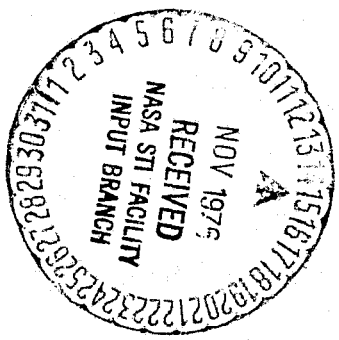

MODE I STRESS INTENSITY FACTORS FOR ROUND COMPACT SPECIMENS

by Bernard Gross
Lewis Research Center
Cleveland, Ohio 44135

TECHNICAL PAPER to be presented at
Task Group E-24. 01. 12 of Committee E-24 of the
American Society for Testing and Materials
Philadelphia, Pennsylvania, October 5, 1976

MODE I STRESS INTENSITY FACTORS FOR ROUND COMPACT SPECIMENS

by Bernard Gross*

ABSTRACT

Mode I stress intensity factors K_I were computed for round compact specimens by the boundary collocation method. Results are presented for ratios A_t/R_o in the range 0.3 to 0.8, where A_t is the distance from the specimen center to the crack tip for a specimen of diameter $2R_o$.

INTRODUCTION

ASTM Standard Method of Test E 399 for Plane Strain Fracture Toughness of Metallic materials is presently confined to two rectangular shaped specimens: bend or compact [1].

In order to economize on test specimen stock and machining for testing of structures such as discs and solid cylinders, a round compact specimen is an obvious substitute for the rectangular compact specimen [2-5]. For this reason, and to evaluate existing experimental and finite element results on the round compact specimen, an independent analytical study was made. The method employed is quite versatile in that a range of load line locations can be assigned and results derived by the superposition of two independent solutions obtained by the boundary collocation method with 60 boundary stations and an overdetermined system of equations as detailed in Ref. 6.

APPROACH

Figure 1(a) shows a cracked round compact specimen, of diameter $2R_o$, loaded through pins by opposed tensile forces P, normal to the crack. The line of action of the load is offset by the distance X_o from the center of the specimen. The analytical solution to this configuration is based on the model shown in Fig. 1(b). There are two independent variables X_o/R_o and A_t/R_o, where A_t is the distance measured from the center of the model to the crack tip.

The analysis follows that of a previous paper on cracked ring segments [7], in that the loading of the specimen is characterized by the statically equivalent combination of resultant force P, chosen to act through the mid-net section, and complementary couple M, as shown in Fig. 2. For the cracked ring segment there is an additional independent parameter R_i/R_o, where R_i is the inner radius. The approach taken here was to estimate the limit of the stress intensity coefficients (defined in Ref. 7) Γ_P and Γ_M as $R_i/R_o \to 0$, in the expectation that these limits would represent appropriate values for the round compact specimen.

It is necessary to consider the limitations of applicability of the present results to practical specimens which are loaded by opposed tensile forces acting through pins. If the crack tip is sufficiently close to the load line, the difference between the actual distribution of loading forces and that assumed in the present analytical model cannot be neglected. Guidance in this respect was obtained from Ref. 8, which deals with the ASTM Standard E399 rectangular compact specimen. For crack length to width ratios less than 0.3, the difference between K_I obtained from an assumed simple boundary load condition as used here and one which models the localized pin loading, becomes significant. One may compare the two speci-

*Lewis Research Center, Cleveland, Ohio, U.S.A.

men types on the basis of the same relative crack lengths (a/W for the rectangular compact specimen and A_t/R_o for the round compact specimen). This is shown in Fig. 3 where a rectangular compact specimen is superimposed on a round compact specimen. Both specimens have the same relative crack length ratio of 0.3. From this representation and the results of Ref. 8, it is surmised that the analytical results presented will apply to the load line locations $X_o > 0$, and A_t/R_o greater than 0.3.

RESULTS AND DISCUSSION

For the round compact specimen, as shown in Fig. 1, there are two independent variables, X_o/R_o and the relative crack length to outer radius ratio, A_t/R_o. With load P applied at X_o, the mid net section nominal bending moment is $M = P(X_o + (R_o + A_t)/2)$. The ratio σ_M/σ_P algebraically reduces to $3(2X_o/R_o + A_t/R_o + 1)/(1 - A_t/R_o)$.

The values of Γ_P and Γ_M were obtained using the boundary collocation technique with 60 boundary stations and an overdetermined system of equations as detailed in Ref. 6. The results for the limit case as $R_I \to 0$, were based on examination of the trends shown in Figs. 4 and 5. From this output the estimated limit values in Table I of Γ_P and Γ_M were obtained.

Applying the principle of superposition to the stress intensity factor K, the equation relating the stress intensity coefficients Γ, Γ_P and Γ_M where $\Gamma = K_I/(\sigma_P + \sigma_M)\sqrt{A_t(1 - A_t/R_o)}$ and is derived as

$$\Gamma = \left(\frac{\sigma_P}{\sigma_P + \sigma_M}\right)\Gamma_P + \left(\frac{\sigma_M}{\sigma_P + \sigma_M}\right)\Gamma_M \tag{1}$$

Through algebraic manipulation one obtains

$$\left(\frac{\sigma_P}{\sigma_P + \sigma_M}\right) = \frac{1 - A_t/R_o}{2(3X_o/R_o + A_t/R_o + 2)} \tag{2}$$

and

$$\left(\frac{\sigma_M}{\sigma_P + \sigma_M}\right) = \frac{3(2X_o/R_o + A_t/R_o + 1)}{2(3X_o/R_o + A_t/R_o + 2)} \tag{3}$$

As shown in Fig. 4, Γ_M converges rapidly with decreasing R_I/R_o ratios. In contrast, Γ_P, Fig. 5 is not as well behaved as Γ_M. However, this uncertainty in Γ_P is not critical since the coefficient of this term in Eq. (1) is small compared with the coefficient of Γ_M (i.e., the specimen is primarily deformed in bending).

Table II shows a comparison of the present results obtained through superposition with the finite element results of Ref. 5 and the experimental results of Refs. 2 and 5. Very good agreement is obtained.

In Ref. 8, for the standard rectangular compact specimen, it was determined that the pin loaded holes can have a significant effect on the stress intensity factor. It is inferred from those results that the analytical results presented here will apply to load line locations $X_o > 0$, and A_t/R_o values greater than 0.3.

NUMERICAL RESULTS

A specific example of using Eq. (1) to obtain the stress intensity coefficient Γ follows.

For $X_o = R_o/2$, one obtains from Eq. (2)

$$\frac{\sigma_P}{(\sigma_P + \sigma_M)} = \frac{1 - A_t/R_o}{(7 + 2\,A_t/R_o)}$$

and from Eq. (3)

$$\frac{\sigma_M}{\sigma_P + \sigma_M} = \frac{6 + 3\,A_t/R_o}{(7 + 2\,A_t/R_o)}$$

For $A_t/R_o = 0.5$, from Table I $\Gamma_P = 0.635$ and $\Gamma_M = 1.02$. Thus,

$$\Gamma = 0.0625(0.635) + 0.9375(1.02) = 0.996$$

CONCLUSIONS

An analytical solution to the model of the round compact specimen (an obvious substitute for the rectangular compact specimen for testing round product forms) has been obtained by the boundary collocation method. Through application of the principle of superposition, the solution for a wide range of load line locations can be obtained. Very good agreement was obtained when compared with available experimental and finite element results for ratios of $A_t/R_o > 0.3$.

Round compact specimens can be used to economize on specimen stock and machining for structures such as discs and solid cylinders.

REFERENCES

1. 1975 Annual Book of ASTM Standards. Part 10-Metals-Mechanical, Fracture and Corrosion Testing; ASTM (1975), pp. 561-580.
2. V. G. Feddern, E. Macherauch: Z. Metallkde, vol. 64, 1973, pp. 882-884.
3. W. Schutz, W. Oberparleiter: AGARD No. 176, Jan. 1974, pp. 370-394.
4. J. H. Underwood, D. P. Kendall: Watervliet Arsenal Rpt. WVT-TR-74041 (1974).
5. D. F. Mawbray, W. R. Andrews: Stress Intensity Calibration for A Compact Specimen With a Round Profile, General Electric Technical Information Series, Jan. 1975.
6. B. Gross, A. Mendelson: Int. J. of Fracture Mechanics, Sept. 1972, vol. 8, no. 3.
7. B. Gross, J. E. Srawley: NASA TM X-71842, 1976.
8. J. C. Newman, Jr: pt. 2, ASTM STP 560, ASTM Phila., Pa., 1974 pp. 105-121.

TABLE I. - ESTIMATED LIMIT VALUES OF Γ_P AND Γ_M AS $R_i/R_o \to 0$

$\frac{A_t}{R_o}$	Γ_P	Γ_M
0.3	0.950	1.41
.4	.720	1.17
.5	.635	1.02
.6	.597	.909
.7	.573	.825
.8	.555	.760

TABLE II. - COMPARISON OF PRESENT RESULTS WITH THOSE OF REFS. 2 AND 5 FOR $X_o/R_o = 0.5$

$\frac{A_t}{R_o}$	Present collocation results, Γ	Experimental results, [2] Γ	Experimental results, [5] Γ	Finite element results, [5] Γ
0.25			1.46	1.44
.30	1.37	1.30		
.40	1.14	1.13	1.12	1.13
.50	.996	1.00		
.55			.936	.929
.60	.894	.874		
.70	.816			.812
.80	.755			

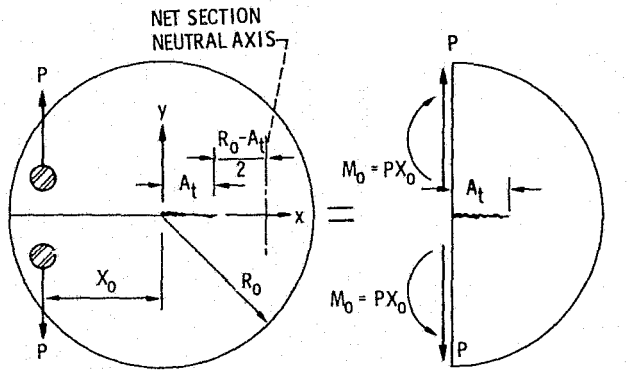

(a) RADIALLY CRACKED SPECIMEN WITH APPLIED P AT X_0.

(b) RADIALLY CRACKED SPECIMEN WITH APPLIED LOAD P AND MOMENT M_0 AT X = 0.

Figure 1. - Load modelling of the round compact specimen.

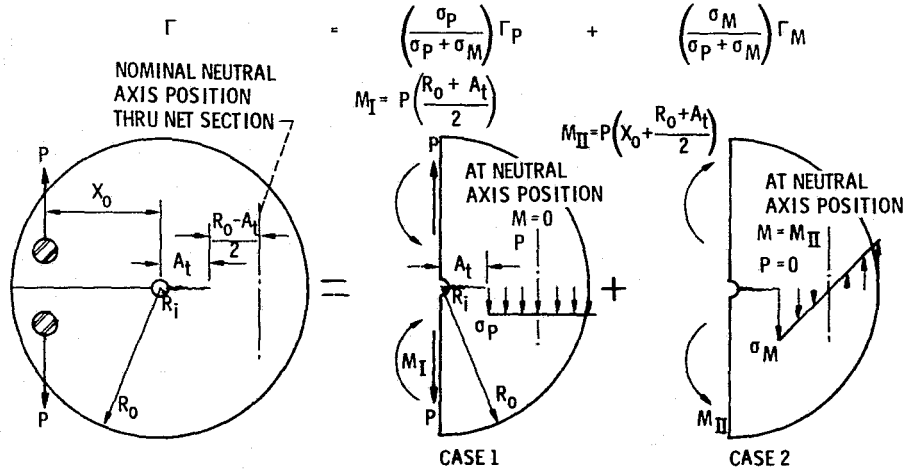

Figure 2. - Application of superposition to round compact specimen loaded through pins at distance X_0, where $\Gamma = \dfrac{K_I}{(\sigma_P+\sigma_M)\sqrt{A_t(1-A_t/R_0)}}$.

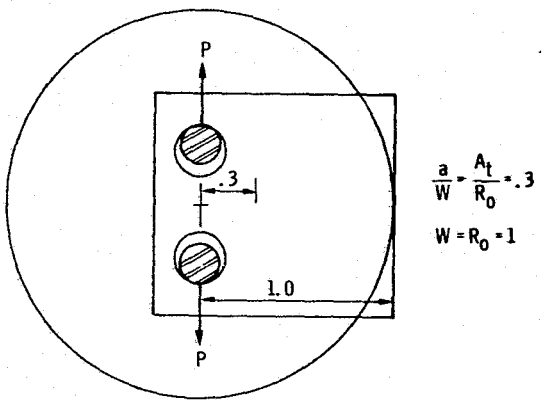

Figure 3. - Round compact specimen superimposed on the rectangular compact specimen for estimating the pin loaded hole effect.

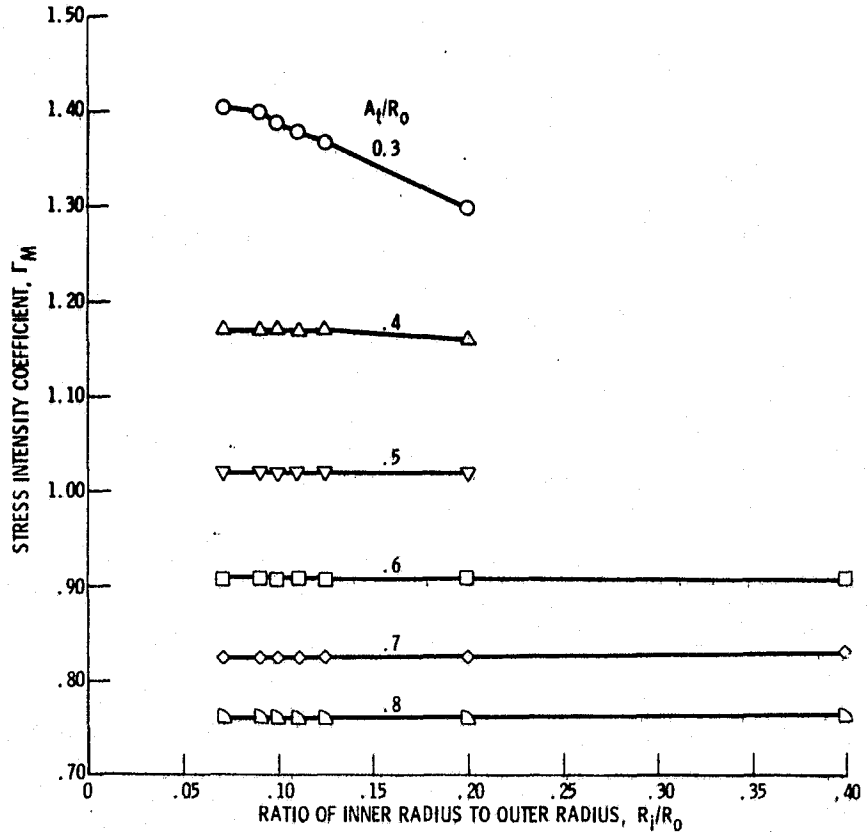

Figure 4. - Convergence of Γ_M with decreasing R_i/R_0 ratios for A_t/R_0 ratios in the range of 0.3 to 0.8.

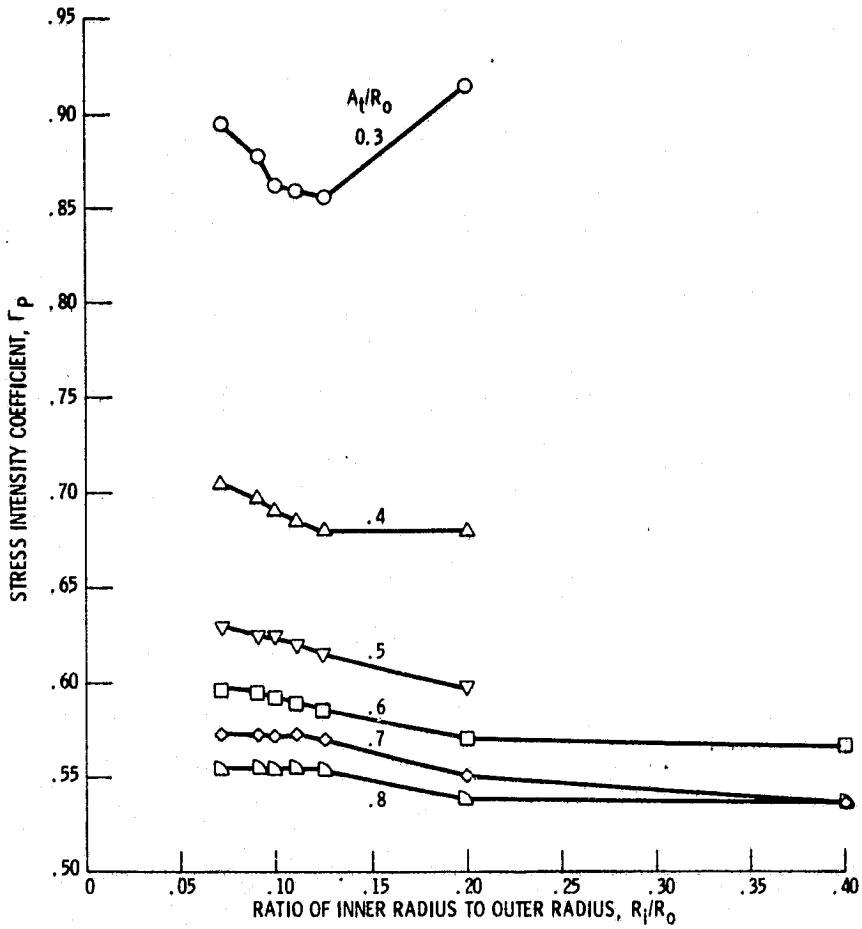

Figure 5. - Convergence of Γ_p with decreasing R_i/R_o ratios for A_t/R_o ratios in the range of 0.3 to 0.8.

NASA-Lewis